Energy Conversion Circuit Laboratory
2023 26th International Conference on Mechatronics Technology (ICMT)

Deadbeat Control for Single-Input Dual-Output Dual Active Bridge Converter

Tan-Quoc Duong
Dept. of Electrical, Electronic and Computer Engineering
University of Ulsan
Ulsan, South Korea
duongtanquoc@gmail.com

Tofopefun Nifise Olayiwola
Dept. of Electrical, Electronic and Computer Engineering
University of Ulsan
Ulsan, South Korea
tofopefungraduate@gmail.com

Tae-Yeong Im
Dept. of Electrical, Electronic and Computer Engineering
University of Ulsan
Ulsan, South Korea
hwaji1@naver.com

Sung-Jin Choi
Dept. of Electrical, Electronic and Computer Engineering
University of Ulsan
Ulsan, South Korea
sjchoi@ulsan.ac.kr

2023 26th International Conference on Mechatronics Technology (ICMT) | 979-8-3503-8142-9/23/$31.00 ©2023 IEEE | DOI: 10.1109/ICMT59920.2023.10373628

***Abstract*—Recently, much attention has been paid to multiport bidirectional isolated DC-DC converters, particularly in power distribution networks and renewable energy sources. The single-input dual-output dual active bridge (DAB) converter can minimize the coupling effect among the inductances of the ports more so than the conventional triple active bridge (TAB) converter by eliminating the inductance on the input port. Therefore, the single-input dual-output DAB converter can function as two separate DAB converters, thereby significantly reducing the complexity of the model-based controller. This study proposes a simple deadbeat control for the single-input dual-output DAB converter under single phase-shift (SPS) modulation. The proposed control does not require any control variables when controlling the voltage at the output port. The proposed method's efficacy is demonstrated and validated through simulation in various operation scenarios.**

Keywords—Dual active bridge converter, Deadbeat control, single phase-shift modulation.

I. Introduction

The multiport bidirectional isolated DC-DC converters have attracted much interest due to their numerous advantages, such as high conversion gain and power density [1]–[8]. By removing the inductance on the input port, the single-input dual-output dual active bridge (DAB) converter can eliminate the coupling effect among the inductances compared to the conventional triple active bridge (TAB) converter. Hence, the energy routing of the single-input dual-output DAB converter is quite comparable to the energy routing of the conventional DAB converters [9].

In addition, the single-input dual-output DAB converter has been the subject of significant research because of its many benefits, including galvanic isolation, ultrafast response, and high efficiency. In general, phase-shift modulation methods appeal to the single-input dual-output DAB converter because of their wide range of applications. Four different types of phase-shift modulation methods, the single phase-shift (SPS), the extended phase-shift (EPS), the dual phase-shift (DPS), and the triple phase-shift (TPS), have been suggested. When the direction of the power flow is altered, it does not have the same effect on the operating states of the two bridges used in EPS. In addition, the EPS and the DPS need two control variables to be implemented. On the other hand, in practical implementation, TPS modulation is the most challenging, returning with three control variables. Therefore, it is easy to explain that one of the most straightforward modulation methods is known as SPS since it is very popular and simple. As a result, SPS is a way of modulation that is generally ideal for ease of implementation with only one control variable in this study [10], [11].

Many control methods based on the modeling of the power converter have been investigated. Among them, deadbeat control is considered one of the most effective methods for controlling the voltage [12], [13]. In addition, the deadbeat control does not require using any control variables, which results in a considerable burden reduction in the control design. From the abovementioned analysis, this study proposes a simple deadbeat control to control the voltage at the output port of the single-input dual-output dual active bridge (DAB) converter SPS modulation.

The remainder of this study has been divided into the following sections after the introduction. Section II details the proposed deadbeat control for the single-input dual-output DAB converter under SPS modulation. The phase-shift duty ratio is derived directly from the system parameters and measured values to control the voltage at the output port. In Section III, simulation results in various operation scenarios will be carried out to illustrate how effective the proposed method is. Finally, Section IV will conclude the efficacy of the proposed method and discuss possible future works.

II. Deadbeat Control for the Single-Input Dual-Output DAB Converter

This section will construct a simple deadbeat control for the single-input dual-output DAB converter with the reduced-order model in a straightforward approach.

Fig. 1 shows the topology of the single-input dual-output DAB converter. It consists of three active bridges, including switches S_{ij} ($i = 1 \sim 4$, $j = 1 \sim 3$), two inductances L_2 and L_3, and the three-winding transformer with the turn ratio $n_1 : n_2 : n_3$. The inductances are composed of the leakage transformer inductances and the additional inductances. C_1,

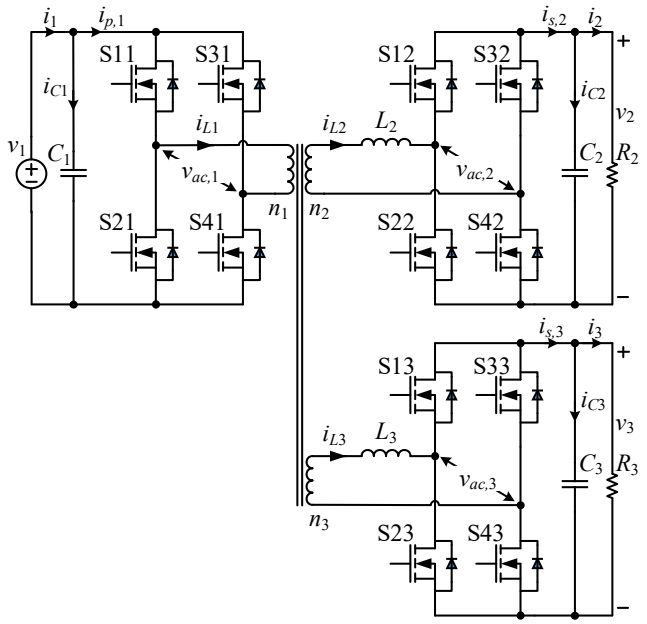

Fig. 1. Topology of the single-input dual-output DAB converter.

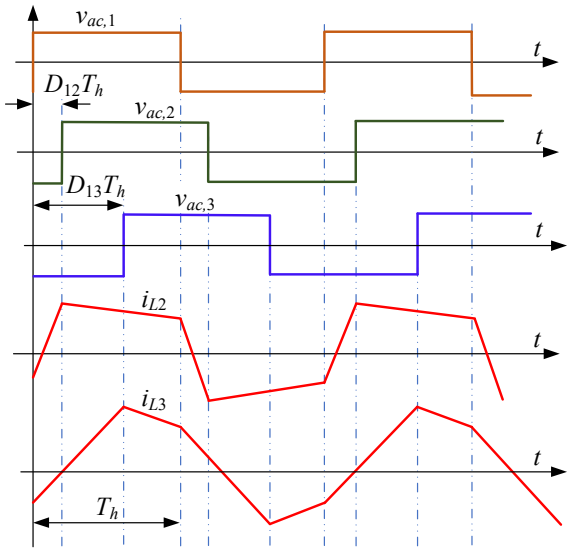

Fig 2. Waveforms of the single-input dual-output DAB converter under SPS modulation.

C_2, and C_3 are the capacitors at the ports. All switches of the converter operate at switching frequency f. The half-switching period $T_h = T/2 = 1/(2f)$, and T is the switching period. Waveforms of the single-input dual-output DAB converter operating under SPS modulation are shown in Fig. 2.

According to Fig. 2 and [14], P_{12} is defined as the transferred power from v_1 to v_2 and P_{13} is defined as the transferred power from v_1 to v_3, which can be calculated with the reduced-order model as shown in (1).

$$P_{1j} = \frac{n_{1j} v_1 v_j}{2fL_j} D_{1j}\left(1 - D_{1j}\right), \quad j = 2,3 \tag{1}$$

where $n_{1j} = n_1/n_j$ and the phase-shift duty ratio D_{1j} determines the transferred power P_{1j}. When D_{1j} is between 0 and 1, the power is transferred with a maximum value at $D_{1j} = 1/2$.

Thus, the corresponding secondary current $i_{s,j}$ in the steady state can be shown in (2).

$$i_{s,j} = \frac{n_{1j} v_1}{2fL_j} D_{1j}\left(1 - D_{1j}\right). \tag{2}$$

On the other hand, the dynamic equation at the output port can be written as shown in (3).

$$C_j \frac{dv_j}{dt} = i_{s,j} - i_j. \tag{3}$$

According to the forward approximation, (3) can be written in discretized form at the k^{th} and $(k-1)^{th}$ sampling period as shown in (4).

$$v_j[k] = \frac{i_{s,j}[k-1] - i_j[k-1]}{fC_j} + v_j[k-1]. \tag{4}$$

In order to simplify the analysis, the phase-shift duty ratio D_{1j} is set as $0 < D_{1j} < 1/2$ in this paper. From (2) and (4), the voltage at the output port can be rewritten as shown in (5).

$$v_j[k] = \frac{n_{1j} v_1[k-1]}{2f^2 L_j C_j} D_{1j}[k-1]\left(1 - D_{1j}[k-1]\right) - \frac{1}{fC_j} i_j[k-1] + v_j[k-1]. \tag{5}$$

For controlling the voltage at the output port, (6) is obtained.

$$v_j[k] = v_{j,d}, \tag{6}$$

where $v_{j,d}$ is the desired value of v_j.

From (5) and (6), the value of D_{1j} at the k^{th} sampling period in deadbeat control is calculated as shown in (7).

$$D_{1j}[k] = \frac{1}{2} - \sqrt{\frac{1}{4} + \frac{2f^2 L_j C_j}{n_{1j} v_1[k]}\left(v_j[k] - v_{j,d} - \frac{i_j[k]}{fC_j}\right)}. \tag{7}$$

According to (7), the voltage at the output port v_j is directly controlled by the corresponding D_{1j} after each sampling period. Obviously, D_{1j} only requires the system parameters and measured values. In addition, the proposed deadbeat control does not necessitate any control variables, which results in a relatively easy controller for implementation.

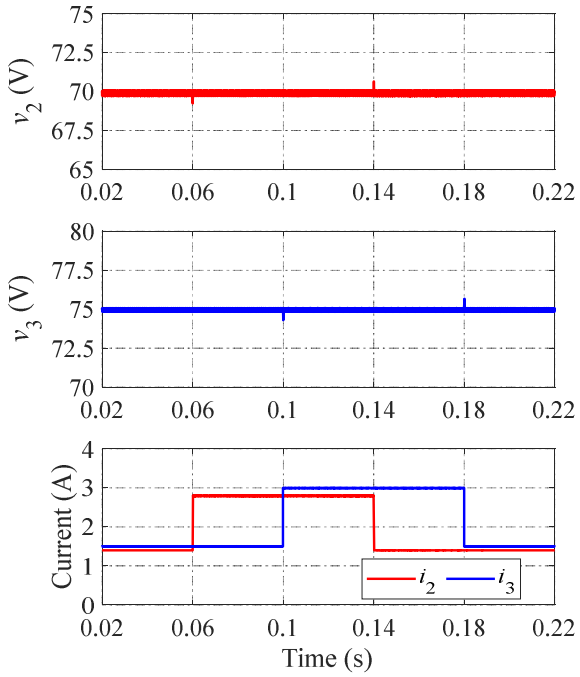

Fig. 3. Simulation results when the resistive loads step up and down between 50 Ω and 25 Ω.

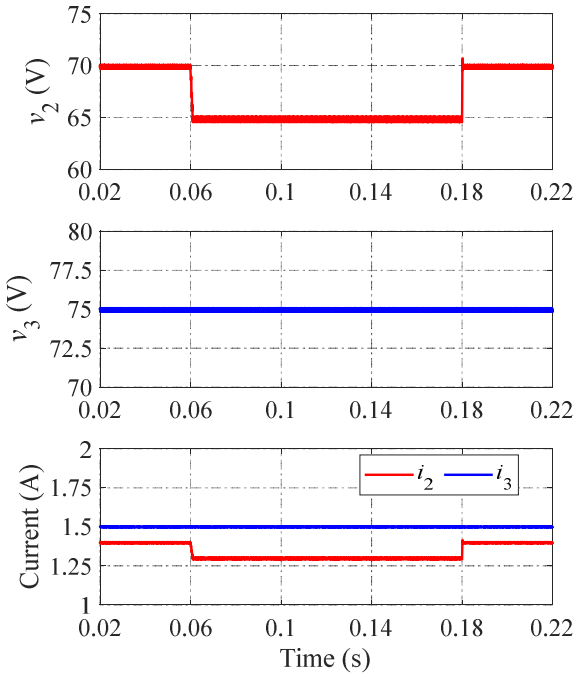

Fig. 4. Simulation results when $v_{2,d}$ changes between 70 V and 65 V.

TABLE I. SIMULATION PARAMETERS

Parameter	Symbol	Value
Switching frequency	f	10 kHz
Port 2 inductance	L_2	50 µH
Port 3 inductance	L_3	50 µH
Port 1 capacitance	C_1	220 µF
Port 2 capacitance	C_2	220 µF
Port 3 capacitance	C_3	220 µF
Port 1 voltage	v_1	80 V
Port 2 voltage	v_2	70 V
Port 3 voltage	v_3	75 V
Transformer turn ratio	n_1:n_2:n_3	1:1:1
Port 2 load	R_2	25 ~ 50 Ω
Port 3 load	R_3	25 ~ 50 Ω

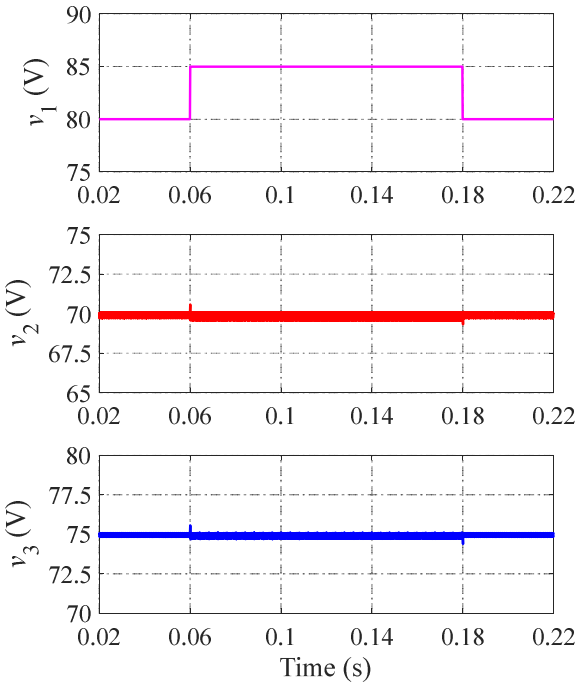

Fig. 5. Simulation results when v_1 increases and decreases between 80 V and 85 V.

III. SIMULATION RESULTS

In this section, the efficacy of the proposed method will be demonstrated by showing simulation results in various operation scenarios. The simulation parameters of the converter are shown in Table I.

Fig. 3 shows the simulation results of the proposed method when the resistive loads R_2 and R_3 step up and down between 50 Ω and 25 Ω. It is easy to see that the voltage at the output port v_2 maintains its desired value with excellent dynamic performance when the current suddenly increases and decreases at 0.06 s and 0.14 s, respectively. For v_3, it shows the same quality of performance as well. In addition, the single-input dual-output DAB converter can function as two separate DAB converters, meaning that the voltages at the output ports do not affect each other, as shown at 0.06 s and 0.1 s when the current is increased and at 0.14 s and 0.18 s when the current is decreased.

Fig. 4 shows the simulation results of the proposed method when $v_{2,d}$ changes between 70 V and 65 V. Clearly, the voltage at the output port v_2 shows excellent dynamic performance. Besides, the voltage at the output port v_3 is not affected by sudden changes in v_2 also.

Fig. 5 shows the simulation results of the proposed method when the voltage at the input port v_1 increases and decreases between 80 V and 85 V. It is easy to see that the voltages at the output ports v_2 and v_3 demonstrate the same excellent dynamic performance. That proves the effectiveness of the proposed deadbeat control.

IV. Conclusions and Future Works

This study proposed a simple deadbeat control for the single-input dual-output DAB converter under SPS modulation. The phase-shift duty ratio is directly derived after each sampling period and only necessitates the system parameters and measured values, resulting in a significantly simple controller for implementation. Various operation scenarios of the converter are utilized to verify the efficacy of the proposed method.

Hardware experiments will further validate the proposed method's efficacy in future studies. Moreover, other modulation techniques could also vary the proposed concept with greater efficacy by minimizing the peak inductor current, expanding the zero voltage switching (ZVS) range, and reducing the backflow power. In addition, the bidirectional mode of the converter will be studied further to enhance the proposed concept.

Acknowledgment

This result was supported by Regional Innovation Strategy (RIS) through the National Research Foundation of Korea (NRF), funded by the Ministry of Education (MOE) (2021RIS-003).

References

[1] H. Yu, Y. Wang, H. Zhang, and Z. Chen, "Impedance Modelling and Stability Analysis of Triple Active Bridge Converter-Based Renewable Electricity-Hydrogen-Integrated Metro DC Traction Power System," *IEEE Trans. Ind. Electron.*, vol. PP, pp. 1–12, 2023.

[2] X. Yu, Z. Lan, J. Zeng, C. Tu, and D. He, "Time-Domain-Based Superposition Analysis for Triple Active Bridge and Its Application for ZVS and Current Stress Optimization," *IEEE Trans. Power Electron.*, vol. 38, no. 5, pp. 5844–5857, 2023.

[3] Y. Wu *et al.*, "A 150-kW 99% Efficient All-Silicon-Carbide Triple-Active-Bridge Converter for Solar-Plus-Storage Systems," *IEEE J. Emerg. Sel. Top. Power Electron.*, vol. 10, no. 4, pp. 3496–3510, 2022.

[4] T. Ohno and N. Hoshi, "Current Tracking Control of Triple Active Bridge DC/DC Converter Under Varying DC-Bus Voltage Conditions," *IEEE Open J. Power Electron.*, vol. 3, no. August, pp. 834–845, 2022.

[5] Y. Qi, X. Liu, W. Li, Z. Zhou, W. Liu, and K. Rajashekara, "Decentralized Control for a Multi-active Bridge Converter," *IEEE Trans. Ind. Electron.*, vol. PP, pp. 1–10, 2022.

[6] J. Li, Q. Luo, T. Luo, D. Mou, and M. Liserre, "Efficiency Optimization Scheme for Isolated Triple Active Bridge DC-DC Converter With Full Soft-Switching and Minimized RMS Current," *IEEE Trans. Power Electron.*, vol. 37, no. 8, pp. 9114–9128, 2022.

[7] A. A. Ibrahim, T. Caldognetto, D. Biadene, and P. Mattavelli, "Multidimensional Ripple Correlation Technique for Optimal Operation of Triple Active-Bridge Converters," *IEEE Trans. Ind. Electron.*, vol. PP, pp. 1–10, 2022.

[8] N. Naseem and H. Cha, "Triple-Active-Bridge Converter With Automatic Voltage Balancing for Bipolar DC Distribution," *IEEE Trans. Power Electron.*, vol. 37, no. 7, pp. 8640–8648, 2022.

[9] P. Gunawardena, N. Hou, and Y. Li, "Decoupling Power Sharing Control Scheme with the Fast Dynamic Response for a Dual-input Dual-active-bridge DC-DC Converter Topology," *2023 IEEE Appl. Power Electron. Conf. Expo.*, pp. 2084–2089, 2023.

[10] B. Zhao, Q. Song, W. Liu, and Y. Sun, "Overview of dual-active-bridge isolated bidirectional DC-DC converter for high-frequency-link power-conversion system," *IEEE Trans. Power Electron.*, vol. 29, no. 8, pp. 4091–4106, 2014.

[11] N. Hou and Y. W. Li, "Overview and Comparison of Modulation and Control Strategies for a Nonresonant Single-Phase Dual-Active-Bridge DC-DC Converter," *IEEE Trans. Power Electron.*, vol. 35, no. 3, pp. 3148–3172, 2020.

[12] S. Wei, Z. Zhao, K. Li, L. Yuan, and W. Wen, "Deadbeat Current Controller for Bidirectional Dual-Active-Bridge Converter Using an Enhanced SPS Modulation Method," *IEEE Trans. Power Electron.*, vol. 36, no. 2, pp. 1274–1279, Feb. 2021.

[13] S. Dutta, S. Hazra, and S. Bhattacharya, "A digital predictive current-mode controller for a single-phase high-frequency transformer-isolated dual-active bridge DC-to-DC converter," *IEEE Trans. Ind. Electron.*, vol. 63, no. 9, pp. 5943–5952, 2016.

[14] S. Shao *et al.*, "Modeling and Advanced Control of Dual Active Bridge DC-DC Converters: A Review," *IEEE Trans. Power Electron.*, 2021.